Caballero Briones, F.; Zapata Navarro, A.; Martel, A.; Iribarren, A.; Peña, J. L.; Castro Rodríguez, R.;
Bartolo Pérez, P.; Rábago Bernal, F.; Jiménez Sandoval, S.

Compositional mixture in R.F. sputtered CdTe oxide films. Raman spectroscopy results

F. Caballero-Briones and A. Zapata-Navarro.
CICATA-IPN Unidad Altamira
Km 14.5 Carretera Tampico-Puerto Industrial Altamira, 89600 Altamira, Tamps., México.

A. Martel and A. Iribarren
Facultad de Física-IMRE Universidad de La Habana
Vedado 10400. La Habana, Cuba

J. L. Peña, R. Castro-Rodríguez and P. Bartolo-Pérez
Departamento de Física Aplicada, CINVESTAV-IPN Unidad Mérida
AP 73 Cordemex, 97310 Mérida, Yuc., México

F. Rábago-Bernal
Instituto de Física, Universidad Autónoma de San Luis Potosí
Av. Alvaro. Obregón 64, 78000, San Lus Potosí, SLP., México

S. Jiménez-Sandoval
CINVESTAV-IPN Unidad Querétaro
AP 1-798, 76001 Querétaro, Qro., México

In this work, radiofrequency sputtered CdTe oxide (CdTeO) films with different oxygen contents were studied by Raman spectroscopy. In films with oxygen contents minor than 0.37 at., we observed bands associated with the LO and 2LO modes of CdTe. As oxygen content increases up to 0.60 at., they appear bands related with $[TeO_3]^{-2}$ trigonal pyramids and with $[TeO_4]^{-4}$ trigonal bipyramids, similar to those reported by other authors in metal-oxide doped TeO_2 glasses. Some additional peaks beyond 750 cm^{-1}, that we have related with $[CdO_6]^-$ polyhedra and with $Cd_xTe_yO_z$ compounds, were observed in that films. We conclude that films evolve from crystalline CdTe to a glassy material where a mixture mainly composed of Te, Cd-Te, $[TeO_3]^{-2}$ and $[TeO_4]^{-4}$, structural units is formed as the oxygen content in the films increases from 0.15 at. to about 0.60 at. fraction.

Keywords: Glasses; Amorphous semiconductors-infrared and Raman spectra; Auger spectroscopy; Thin films growth; structure; and epitaxy
PACS: 61.43.Fs; 78.30.L; 82.80. P; 68.55

1. Introduction

Amorphous CdTe oxide (*a*-CdTeO) thin films have been studied in the last decade because of its potential applications in the optoelectronic and solar cell industries where they may play a role in the fabrication of CdTe-based devices, similar to that of amorphous SiO_2 in silicon-based devices [1]. The optical properties of *a*-CdTe:O films have shown that the optical energy gap can be tuned between 1.48 eV and 3.35 eV by controlling the oxygen content of the films [2].

CdTeO films are currently prepared by rf reactive sputtering, using an Ar-N_2 plasma, which is thought to catalyze the CdTe oxidation by the residual or added oxygen [1-3], or using a highly oxidizing gas such as N_2O [4-6]. Within this method, amorphous films with oxygen contents between 0.07 and 0.60 at. are typically obtained with the substrate at room temperature. In post-annealed CdTeO films has been found evidence of crystalline phases

such as $CdTeO_3$ and $CdTe_2O_5$; however, the structure of the as-deposited films has been difficult to elucidate.

In previous works [4,5] we had shown that the oxygen incorporation causes a change in the Te valence from Te^{-2} to Te^{+4}. We proposed that the simultaneous presence of Te^{-2} and Te^{+4} causes a mixed compound structure in the middle-oxygen region, where the films will be composed by Cd-Te and $[TeO_4]^{-4}$ molecular subunits [6]. It was proposed that $[TeO_4]^{-4}$ subunit formation is aleatorious and causes the amorphization of the films [6].

Raman spectroscopy is a very sensitive technique to local order. It has been used to monitor the crystalline quality in II-VI semiconductors [7,8] and to study the structure of telluritic glasses (TeO_2) doped with different metal-oxides (MO) [9-13], but to the best of our knowledge, few Raman works are published in amorphous or microcrystalline films.

In the present work we study *a*-CdTeO films by Raman spectroscopy. The observed bands were related to those
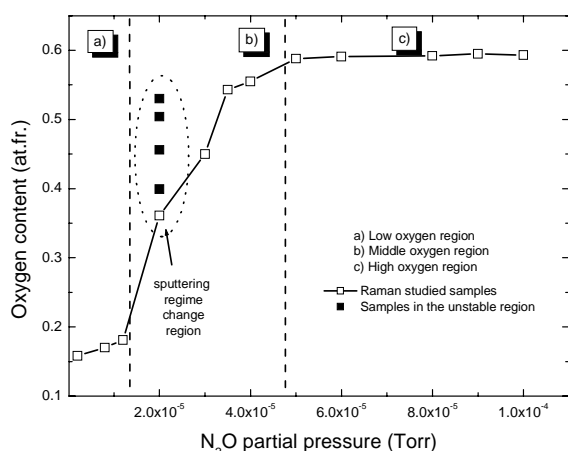
Corresponding author. E-mail fcaballero@ipn.mx, Tel & Fax 01 833 2600125

Figure 1. Oxygen contents in the films vs N_2O partial pressures used
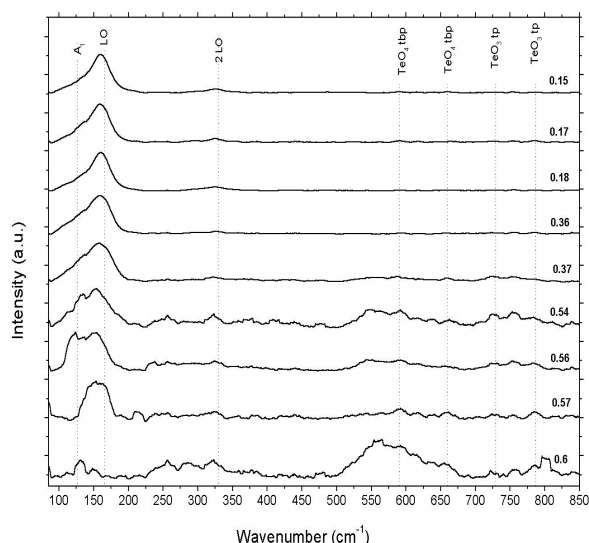

Figure 2. Normalized intensity Raman spectra of films with different oxygen content. The oxygen content is pointed at the right of each curve.
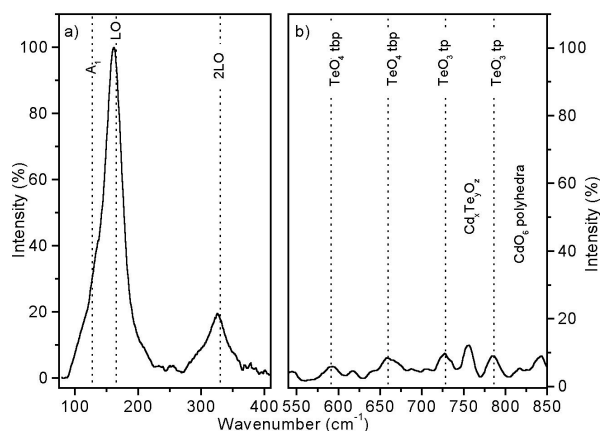

Figure 3. Typical Raman spectrum at low oxygen content. a) CdTe peak region. b) Glass peak region.

observed in CdTe and MO-doped TeO_2 glasses, and compared with our previous results.

2. Experimental procedures

The films were prepared in a CVE 301 (Cooke Vacuum Products) sputtering system with a US Gun II magnetron powered by a rf source from Advanced Energy Products. We used a 25 mm diameter CdTe target, pressed from 99.999% purity CdTe powder (Cerac). 99.999% purity Ar (Linde) and N_2O (MG industries) were used as working gases. Films were deposited onto 12 x 12 mm, degreased and ultrasonically cleaned Corning glass slides. The substrate holder temperature was kept constant at 50º C. The deposition time was 15 minutes. The total working pressure was 2×10^{-2} Torr and the plasma power was 30 W. Films were growth at different N_2O partial pressures, first introducing the N_2O with a variable leak valve (Granville Phillips) to reach the desired N_2O pressure as measured by a hot cathode vaccuometer (Granville Phillips) and then completing with Ar to the working pressure. Before the film deposition the target was Ar-presputtered for 5 minutes. The films were highly adherent, showing with increasing oxygen content, gradual colour change from gray to transparent. The obtained films present thicknesses between 0.8 and 1.5 µm. Thickness decreases when the partial pressure of N_2O increases.

The oxygen content of the samples was determined by AES in an ESCA/SAM PHI 560 from Perkin Elmer, using the previously reported oxygen sensitivity factor [4]. Before analysis, the samples were eroded 1 min with a 2 keV Ar^+ beam.

The Raman measurements were carried out at room temperature in a Labram Dilor micro Raman system using a 632.8 nm He-Ne laser and a low-noise thermoelectrically cooled CCD detector. The laser spot diameter on the sample surface was 2 µm and neutral density filters were used to avoid sample changes produced by laser heating effects. Similar spectra were obtained through the entire surface of the sample.

3. Results and discussion

In the Figure 1 are shown the oxygen atomic fractions of the films obtained at the different N_2O pressures used. Films with oxygen contents between 0.16 and 0.59 at. fr. were obtained, when increasing the N_2O pressure. An important increase in the oxygen content is observed above 1×10^{-5} Torr, as the Te^{-2} in CdTe changes its valence to Te^{+4} [4-6]. The points inside the circled zone are samples grown at equal conditions, but having very different oxygen concentrations. This is due to the change in the sputtering regime in this region, where it is difficult to obtain controllable films [14]. At N_2O pressures above this unstable region, the oxygen contents in the films increases smoothly, to finally reach values close to the stoichiometric saturation of CdTe i.e. 0.60 at. fr.. This behaviour defines roughly three regions, as seen in the Figure: the low, the
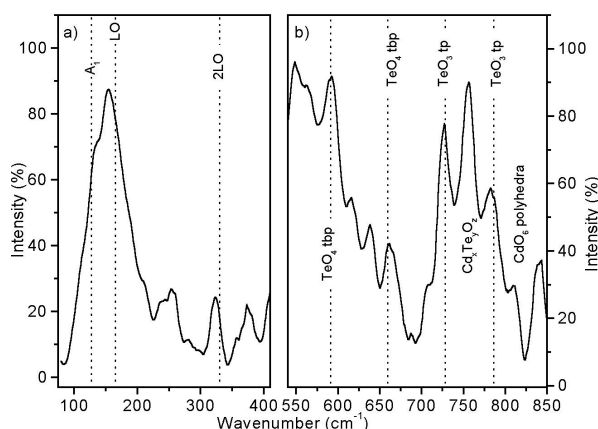
Figure 4. Typical Raman spectrum at middle oxygen content. a) CdTe peak region. b) Glass peak region.

Figure 5. Typical Raman spectrum at high oxygen content: a) CdTe peak region. b) Glass peak region.

middle and the high oxygen regions, related to the amount of Te^{+4} present in the films. A more detailed discussion of the oxygen incorporation mechanisms to CdTeO films will be subject of a future work.

The films were studied using Raman spectroscopy. The signal/noise ratio of the raw spectra falls at high wavenumbers when the oxygen content increases. Such behaviour can be related to the film composition evolution from CdTe-like compounds to Glass-like ones when the oxygen content increases. The background has a reverse behaviour, increasing at high wavenumbers when the oxygen content in the films increases. It is known [7] that the background is not a negligible part in the Raman scattering signal since it arises from multiple order scattering or fluorescence, and must be taken into account for quantitative measurements. Nevertheless, in the results described here, a qualitative description of the main features is considered sufficient.

The spectra shown in Figure 2 were background-subtracted by applying a polynomial function, and normalized to the maximum value. The oxygen atomic fraction of the films increases from the top to the bottom. The spectra will be analysed within two regions named in this work CdTe-like region, below 400 cm^{-1} and Glass-like region, above this value. In the CdTe region are labelled three bands, related to CdTe and to hexagonal Te. In the Glass region we identified a set of bands related to tellurite glasses. For the assignment of the bands we used the values reported in refs. [8-13] as shown in Table I.

It is important to point out that the peak positions on the Raman bands in telluritic glasses move in relative wide limits depending on the cation type and its concentration [10,15]. Mean positions will appear in dotted line in all figures. We did not find evidence of SiO_2 related bands, indicating that films are thick enough to avoid glass substrate detection.

In Figure 2 it can be seen that the films with less than 0.37 oxygen content present well defined features related to the LO and 2LO bands of CdTe. The next samples, i.e. 0.54–0.57 O at. fr., show the above mentioned LO and 2LO
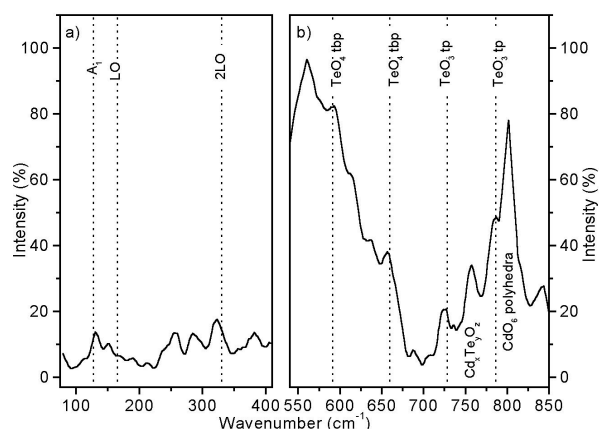
CdTe bands and a band related with the Te A_1 mode. It also appears a wide band about 500-700 cm^{-1} associated with $[TeO_4]^{-4}$ trigonal bipyramids (tbp) and a band between 700-800 cm^{-1} related to $[TeO_3]^{-2}$ trigonal pyramids (tp). The last sample, with 0.59 O at.fr., shows very weak CdTe-related bands, a well-defined 500-700 cm^{-1} band and a more deformed and lower intensity 700-800 cm^{-1} band.

We do not observe bands around 450 cm^{-1} in any sample, which have been related to bending vibrations of the Te-O-Te linkages in a continuous TeO_2 network [9-11].

The results indicate that a CdTe-related structure is present through almost the entire range of oxygen contents, being gradually substituted by an oxidized material that present bands closely related to those reported for tellurite glasses. The absence of the 450 cm^{-1} band confirms that the TeO_2 continuous network of $[TeO_4]^{-4}$ tbp is not formed, as a high Cd concentration is always present [5], but a glassy mixture of Te, Cd-Te, $[TeO_3]^{-2}$ and $[TeO_4]^{-4}$ molecular subunits interlinked. CdTe in microcrystalline form can be assumed as the LO modes are clearly defined. The Te presence could be explained in terms of Te aggregates, frequently found in CdTe films, especially when growth on amorphous substrates [8]. The amount of such aggregates could be very small, but relative high-level signals are obtained due to the strong resonance in the Raman effect when Te crystals are excited by laser radiation of about 2 eV [16].

By the other hand, it is well known that the frequency and temperature factor of the intensity of a Raman Peak is given by the expression [17,18]:

$$ R = cte \; \frac{[\upsilon_o + \upsilon]^4}{\upsilon} \frac{1}{1 - \exp\left[-\dfrac{h\upsilon}{k\,T}\right]} \tag{1} $$

where $\mathbf{\upsilon_o}$ and $\mathbf{\upsilon}$ are the frequencies of the exciting laser and the scattered light, respectively, k the Planck constant and T the sample temperature.

Following to other authors [12,19] we performed the

Table 1. Literature review of Raman band assignments for Te, CdTe and binary telluritic glasses [8-13].

Band ID	Wavenumber (cm^{-1})	Vibration mode
A$_1$	125	Phonon vibrations -Te structure
LO	165	Phonon vibrations - CdTe structure
2LO	325	Phonon vibrations - CdTe structure
A	770-780	Stretching vibrations-TeO$_3$ tp
B	720-760	Stretching vibrations -TeO$_3$ tp
C	650-670	Stretching vibrations - TeO$_4$ tbp
D	600-615	Stretching vibrations TeO$_4$ tbp
E	400-500	Bending vibrations -[Te-O-Te] or [O-Te-O] linkage

temperature-frequency correction, i.e. after background subtraction; the spectrum is divided by the factor R. The correction is a non-linear transformation of the spectrum, which will have the greatest effect in the lower-wavenumber portion of spectra. This region will be intensity-compressed and the positions of peaks will slightly move toward higher wavenumbers. The procedure is similar to the k^2-weighing performed to the EXAFS spectra to amplify the oscillations at high k [20].

Figure 3 shows the corrected Raman spectrum of the sample with 0.18 oxygen atomic fraction. This spectrum is typical of the low oxygen region: **a)** At wavenumbers <400 cm^{-1}, it can be seen well-defined LO and 2LO bands of CdTe at about 165 cm^{-1} and 325 cm^{-1} respectively. **b)** The region from 550 cm^{-1} to 800 cm^{-1} shows very weak, noisy bands. This result indicates that film consists basically of CdTe.

Figure 3 shows the corrected spectrum of the sample with 0.54 oxygen atomic fraction, which corresponds to the middle oxygen content region. **a)** Between 100-400 cm^{-1} it can be noticed that the CdTe 2LO region is worse defined and weaker, suggesting a less ordered material. The Te A$_1$ peak can be distinguished here as a shoulder in the 100-200 cm^{-1} region. **b)** The region >500 cm^{-1} shows clearly defined [TeO$_4$]$^{-4}$ tbp bands, at about 590 and 660 cm^{-1} and [TeO$_3$]$^{-2}$ tp bands at about 720, 780 cm^{-1}. Sekiya *et al.* [13] investigated the Raman spectra of M$_x$Te$_y$O$_z$ (M = Ba, Mg, Zn) crystals and found main peaks between 725 and 790 cm^{-1} that they assigned these to the stretching vibration between Te and non-bridging oxygen atoms. Following Sekiya, the feature at about 750 cm^{-1} could be related with Cd$_x$Te$_y$O$_z$ microcrystalline compounds [13]. Compared with the spectrum in Figure 3, it can be seen that the intensity of the bands in the Glass region is similar with the CdTe region. These results indicate that Cd-Te bonding is leading place to an aleatorious mixture of tellurium coordination states that are responsible for the loss of crystalline ordering of the films. The Figure also shows a feature at about 800 cm^{-1} that can be related to Cd-O bonding which is analyzed below.

Figure 5 displays the corrected spectrum of the sample with 0.59 oxygen atomic fraction, near the stoichiometric saturation of CdTe, i.e. 0.60 at. fr., (all Te in Te^{+4} state). The figure shows: **a)** a drastic reduction of the bands in the <400 cm^{-1} region due to the global decreasing of the CdTe

phase. A very doubtful evidence of Te A$_1$ band can be noted, indicating that Te-Te bonds are practically not present. **b)** The predominance of the Glass region bands is clear in this spectrum, as expected with the increasing of the Te-O bonding. Here, all the above-mentioned features, i.e. the [TeO$_4$]$^{-4}$ tbp, [TeO$_3$]$^{-2}$ tp, and Cd$_x$Te$_y$O$_z$ are present. The feature at about 800 cm^{-1} is stronger and more defined than in the Figure 4. Duverger [11], who has investigated MgO-, PbO- and ZnO-doped TeO$_2$ glasses, has pointed out that it is essential to consider the contribution of the stretching vibration involving dopant metal and oxygen in the band upper 730 cm^{-1}. [ZnO$_6$]$^-$ polyhedra had been found by Kozhukharov *et al.* [21] in ZnO-doped TeO$_2$ glass. Then, the feature at about 800 cm^{-1} could be related to O-Cd-O linkages in [CdO$_6$]$^-$ polyhedra.

In the Figure 5, the [TeO$_3$]$^{-2}$ bands seem to be relatively reduced compared with the Figure 4 spectrum and the [TeO$_{3+1}$] seem to increase. This may be understood as a tendency of the material to form exclusively a [TeO$_4$]$^{-4}$ network, deformed by the Cd presence, however, in the present state of our study we cannot discriminate them by the observed Raman bands.

The above results are consistent with our previous results that show Te changes its valence from Te^{-2} in CdTe to Te^{+4} in CdTeO$_3$, with a mixture of them at the intermediate oxygen contents [4,5]. This change of valence will induce the aleatorious formation of the mentioned molecular subunits, as we have pointed out earlier [6], with the correspondent loss of ordering. Further work will be performed to quantify the amounts of the [TeO$_3$]$^{-2}$, [TeO$_4$]$^{-4}$ and [TeO$_{3+1}$] molecular subunits with respect to the amount of oxygen present and to the Cd to Te bonding in order to get a more detailed description of the structure evolution of this material.

4. Conclusions

We study CdTeO films grown by reactive rf sputtering by Raman spectroscopy and found that they can be described as a mixture of structural subunits such as Cd-Te, [TeO$_3$]$^{-2}$, and [TeO$_4$]$^{-4}$. At low oxygen content CdTe is the dominant material. As Te changes its oxidation state from Te^{-2} to Te^{+4} with increasing oxygen content, [TeO$_3$]$^{-2}$ trigonal pyramids as well as [TeO$_4$]$^{-4}$ trigonal bipyramids are formed, and films tend to a glassy material. We found

some additional peaks beyond 750 cm^{-1} that we related with $[CdO_6]^{-1}$ polyhedra and $Cd_xTe_yO_z$ microcrystalline compounds.

References

[1] F.J. Espinoza-Beltrán, *et al.*, Jap. J. Appl. Phys. **30** 1715 (1991).
[2] F.J. Espinoza-Beltrán, R. Ramírez-Bon, F. Sánchez-Sinencio, O. Zelaya-Angel, G. Torres-Delgado, J.G. Mendoza-Alvarez, J. González-Hernández, M. H. Farías and L. Baños, Braz. J. Phys. **24** 426 (1994).
[3] M.Y. El Azhari, M. Azizan, A. Bennouna, A. Outzourhit, E.L. Ameziane and M. Brunel, Sol. Energy Mater. and Sol. Cells **45** 341 (1997).
[4] Zapata-Navarro, M. Zapata-Torres, V. Sosa, P. Bartolo-Pérez and J.L. Peña, J. Vac. Sci. Technol. A **12** 714 (1994).
[5] Zapata-Navarro, P. Bartolo-Pérez, M. Zapata-Torres, R. Castro-Rodríguez and J.L. Peña, J. Vac. Sci. Technol. A **15** 2537 (1997).
[6] Iribarren, E. Menéndez, R.Castro-Rodríguez, V. Sosa, J.L. Peña and F. Caballero-Briones, J. Appl. Phys. **86** 4688 (1999).
[7] Zwick and R. Charles, Phys. Rew. **48** 6020 (1994).
[8] S. Jiménez-Sandoval, S. López-López, B.S. Chao and M. Meléndez-Lira, Thin Solid Films **342** 1 (1999).
[9] V. R. Chowdari and P. Kumari, Mat. Res. Bull. **34** 327 (1999).
[10] H. Li, Y. Su, S. K. Sundaran, J. Non-Cryst. Solids **402,** 293 (2001).
[11] Duverger, M. Bouazaoui and S. Turrell, J. Non-Cryst. Solids **220** 169 (1997).
[12] Y. Himei, A. Osaka, T. Nanba and Y. Miura, J. Non-Cryst. Solids **177** 164 (1994).
[13] T. Sekiya, N. Mochida and A. Ohtsuka, J. Non-Cryst. Solids **168**, 106 (1994).
[14] M. Yoshitake, T. Yotsuya, S. Ogawa, Japn. J. Appl. Phys. **31**, 4002 (1992)
[15] H. Munemura, K. Mitone, M. Misawa, K. Nayurama, J. Non-Cryst. Solids **700** 293 (2001).
[16] P. M. Amirtharaj and F. H. Pollak, Appl. Phys. Lett. **45** (1984) 402.
[17] W. Kiefer "Raman Spektroskopie". Chapter 5 in "Spectroskopie amorpher und kristaliner Festköper". Eds. D. Haarer and W. Spiess, 115 (1995).
[18] "Vibrational Intensities in Infrared and Raman Spectroscopy". Eds. W. B. Person and G. Zerbi. Elsevier Sciantific Publishing Cpmpany. Amsderdam. (1982).
[19] B. Mysen, L. W. Finger, D. Virgo and F. A. Seifer. Am. Mineral **67** 686 (1982).
[20] M. Newville, "Fundamentals of EXAFS", Consortium of Advanced Radiation Sources, University of Chicago, 19 (2002).
[21] V. Kozhukharov, H. Burger, S. Neov, B. Sidzhimov. Polyhedron, **5** 771 (1986).